UDC 528.852.088-047.44 **doi: 10.32620/aktt.2023.2.07**

Viktor MAKARICHEV, Bogdan KOVALENKO, Vladimir LUKIN

National Aerospace University "Kharkiv Aviation Institute", Kharkiv, Ukraine

PRELIMINARY ANALYSIS OF NOISY IMAGE LOSSY COMPRESSION BY DISCRETE ATOMIC TRANSFORM-BASED CODER

Remote sensing provides data (images) important for many modern applications. Image number and average size tend to increase. This makes their transfer via communication lines, storage, and dissemination problematic. Thus, compression should be applied where lossy compression is mostly used. Most methods of lossy compression assume that images do not contain noise. Meanwhile, images are often noisy, and this should be considered in the design and performance analysis of image compression techniques. Lossy compression has already been studied by several coders. However, it has not been investigated for the recently proposed atomic transform-based techniques that possess several advantages, in particular, the ability to provide privacy of compressed data. The main ***subject*** *of this paper is the peculiarities of noisy image lossy compression by an atomic transform-based coder. Our* ***goal*** *is to analyze whether the considered compression method provides the noise filtering effect and the so-called optimal operation point. The* ***task*** *is to obtain rated distortion curves for the atomic transform-based coder applied to noisy images and to analyze their behavior for several performance characteristics such as quality metrics and compression ratio. In the first order, the monotonicity of the main dependence is of interest. The main* ***results*** *are as follows. First, it is shown that the dependencies have non-monotonic behavior and the appearance of analogs of optimal operation point is possible, at least, for such metric as maximal absolute error. Second, there is a specific dependence of compression ratio on a parameter called UBMAD that controls compression. Experiments have been performed on several noisy test images having different complexity and contaminated by noise of different intensities. In* ***conclusion****, it is demonstrated that one more coder might have optimal operation points for images having a rather simple structure. However, at the moment, it is difficult to predict its existence and the corresponding coder parameters.*

Keywords: *lossy compression; discrete atomic transform; rate-distortion curve; optimal operation point.*

Introduction

Image acquisition from spaceborne and airborne carriers and their further processing have become widespread means for various applications [1, 2]. For useful information extraction from the obtained remote sensing (RS) data, they should be usually passed to on-land centers of data processing and, possibly, stored [3]. However, the problem with RS data transfer via communication lines and their storage is that the data size has an obvious tendency to rapid increase [3]. There are several main reasons behind this – the resolution of imaging systems improve, images are acquired more frequently, and most imaging systems are multichannel [3, 4]. To solve the problem, image compression is widely used [5-7].

Image compression methods can be divided into lossless and lossy [8, 9]. The use of lossless methods is limited since they usually do not provide appropriately large compression ratios (CRs) and, besides, CR cannot be varied. Thus, lossy compression techniques are widely exploited [10-12].

There are various methods of image lossy compression [9, 13, 14] and priorities of requirements to them [11, 15, 16]. Most modern lossy compression techniques are based on orthogonal transforms, mainly discrete cosine transform (DCT) and discrete wavelet transforms (DWTs) [11, 13, 15] although there is also a permanent interest in neural network-based compression [10]. A set of requirements to image lossy compression might include the following:

1) to provide a desired CR [13],

2) to ensure an appropriate trade-off between quality characterized by a given metric and CR [16],

3) to provide a desired quality and make this easily and quickly enough [11],

4) to ensure privacy protection for compressed data [15], etc.

In a practical situation, not all of the aforementioned requirements have to be satisfied simultaneously and their priority can be different. Below, we concentrate on the case when it is desired to provide privacy protection easily and reliably as well as to ensure a reasonably high quality of compressed noisy images.

In this sense, methods of lossy compression based on discrete atomic transform (DAT) [15, 17] have several positive features. First, they provide privacy protection for compressed data. Second, DAT-based compression performs better than JPEG in terms of peak signal-to-

noise ratio (PSNR) for the same compression ratio (CR) for grayscale and three-channel (color) images [15]. Third, DAT-based methods allow for controlling maximal absolute deviation (MAD), which is important in remote sensing applications when image classification is the final goal [18]. Fourth, there are quite strict connections between MAD and standard metrics of image quality such as PSNR that allows relatively easy and fast providing of the desired quality of compressed images [15]. Finally, there are approaches intended to sufficiently decrease the memory expenses at compression and decompression stages [17].

The DAT-based compression methods have been intensively tested for grayscale and color images (see [15, 17] and references therein) where those images did not contain noise or, at least, this noise was invisible. Meanwhile, there are quite many practical situations [19-21] where noise is inevitable or can be quite intensive. Noise is visible in radar images [19] as well as in images acquired in bad illumination conditions [20] or in some component images of hyperspectral remote sensing data [21]. Lossy compression of noisy images has certain peculiarities discovered about 25 years ago [22, 23] and studied later more in detail [24, 25] for coders based on discrete cosine transform (DCT) and wavelets. In particular, specific noise-filtering effect was discovered.

It has been also shown that, due to this effect, optimal operation point (OOP) might exist where OOP is such a parameter that controls compression (PCC) that compression in it provides the maximal similarity between a compressed and the corresponding noise-free (true) images, which is better than for the original (noisy, uncompressed) image. It has been also shown that, even without having the noise-free images, OOP existence and PCC for it can be predicted [24, 25].

Meanwhile, DAT-based compression has been never tried for noisy images, and it is not known does OOP exist for it. Thus, the main goal of this paper is to check if OOP can be observed in the case of DAT-based compression of noisy images and, if yes, what are the initial assumptions concerning the corresponding PCC.

Problem statement

DAT-based compression uses a scheme typical for most wavelet-based compression techniques (Fig. 1). A three-channel (or RGB) image is first decomposed using RGB to YCbCr transform to decorrelate data. Then, DAT is applied component-wise, and the obtained coefficients are quantized and compressed using a combination of Golomb codes and context-adaptive binary arithmetic coding. Decompression is carried out in inverse order. The wavelets are constructed using the atomic function

$$up_s(x)=\frac{1}{2\pi}\int_{-\infty}^{\infty} e^{itx}\prod_{k=1}^{\infty}\frac{\sin^2\left(st(2s)^{-k}\right)}{s^2t(2s)^{-k}\sin\left(t(2s)^{-k}\right)}dt,$$
$$s=1,2,3,...$$

where s is an integer; k is an index, which varies from one to infinity; x is an independent variable; t is an integration variable; i and π are classic mathematical constants. In this study, we consider the case s = 32. We note that, in DAT, non-stationary infinitely locally supported wavelets are applied.

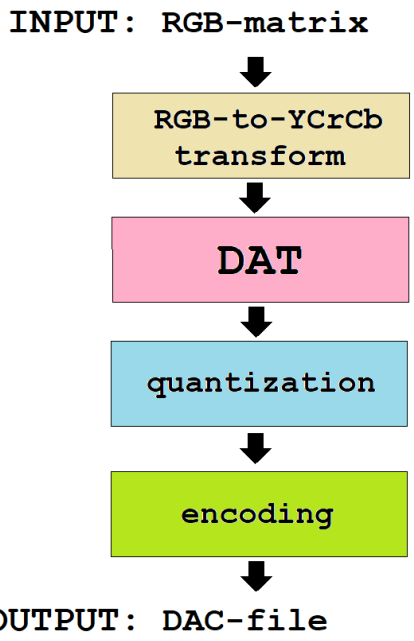

Fig. 1. The block diagram of DAT-based compression

Compression based on DAT is controlled by the so-called upper bound of MAD (UBMAD). A larger UBMAD relates to a larger MAD, larger mean square error (MSE) and CR, and smaller PSNR. Meanwhile, CR also depends on image complexity. Approximate expressions that allow estimating (predicting) MSE or PSNR for a given UBMAD are presented in [15].

Analysis of lossy compression of noisy images has several specific features [23-25]. First, studies are usually carried out using three types of images: noise-free (true) image $\mathbf{I}^t$, noisy image $\mathbf{I}^n$, and compressed image $\mathbf{I}^c$. Then, in fact, it is possible to calculate two types of rate/distortion curves - dependencies of a considered full-reference metric for 1) images $\mathbf{I}^n$ and $\mathbf{I}^c$; 2) images $\mathbf{I}^t$ and $\mathbf{I}^c$. In the former case, one gets traditional dependencies that can be obtained in practice since both $\mathbf{I}^n$ and $\mathbf{I}^c$(PCC) are available. For the latter case, such dependencies can be obtained only in simulations since images $\mathbf{I}^t$ are not available. Because of this, we need to say a few words about the conditions of carrying out simulations.

If some study concerning noise influence on performance of some image processing methods is started, it is commonly assumed that noise is additive, white, and Gaussian (AWGN) [24]. We will do the same supposing that we deal with AWGN with zero mean and variance σ^2 known in advance or pre-estimated with high accuracy. Our goal is to determine do OOP exist and according to what metrics. If a metric is determined for the images $\mathbf{I}^n$ and $\mathbf{I}^c$, the subscript nc will be used. In turn, if a metric is calculated for the images $\mathbf{I}^t$ and $\mathbf{I}^c$, it is marked by the subscript tc.

OOP existence can be considered proven if, according to a given metric $Metr_{tc}$, there is a global maximum for which $Metr_{tc}(PCC_{OOP}) < Metr_{tc}(PCC_{OOP} \to 0)$. Here we assume that the metric value is larger if the similarity is larger (PSNR is an example) and $PCC_{OOP} \to 0$ relates to practically uncompressed images (one example is the quantization step for DCT-based coders and another example is UBMAD for the considered DAT-based compression). Thus, our task is to consider typical rate/distortion curves and to analyze the peculiarities of their behavior for the DAT-based compression. Recall here that, according to previous experience, OOPs are usually observed for simple structure images (containing large homogeneous areas) corrupted by a rather intensive noise. In addition, OOPs are more often observed for such conventional metrics as PSNR compared to visual quality metrics.

Analysis of rate/distortion curves

Keeping in mind the aforementioned property, we have carried out our studies for two images presented in Fig. 2.

Let us start our analysis from the most typical dependencies [9, 11]: the rate-distortion curve MSE_{nc}(UBMAD) and CR(UBMAD). They are presented in Fig. 3. As one can see, they are both a little bit specific. First, a general tendency for MSE_{nc} is that it increases if UBMAD increases. However, there is an MSE_{nc} small jump for UBMAD=48 and the dependence is not monotonous – there is a small decrease of MSE_{nc} when UBMAD is about 350. Besides, MSEnc increases slower (nonlinearly) for larger UBMAD. Note that in this paper we consider UBMAD values that have not been earlier studied in [15] and other our paper that dealt with DAT-based compression mostly in the visually lossless mode (for $PSNR_{nc}$ larger than 33-35 dB, i.e. MSE smaller than 20-30).

Dependencies CR(UBMAD) are specific too. They have some "flat" intervals where UBMAD increase does not lead to CR increase. This shows that it is a little bit problematic to set a proper UBMAD to provide a desired CR or MSE_{nc} even if one uses a two-step procedure [11]. This also means that dependencies MSE_{nc}(UBMAD) and CR(UBMAD) should be studied in the future more in detail, especially for large UBMAD values.

Meanwhile, we are more interested in studying the dependencies $Metr_{tc}$(UBMAD). Two of them are presented in Fig. 4 (let us start by considering the case of AWGN with noise variance equal to 100). The first is $PSNR_{tc}$(UBMAD) and the second one is $PSNR\text{-}HA_{tc}$(UBMAD). Recall here that PSNR-HA is a visual quality metric [26] that has larger values if compressed image quality is better. Similarly, to PSNR, PSNR-HA is expressed in dB.

a

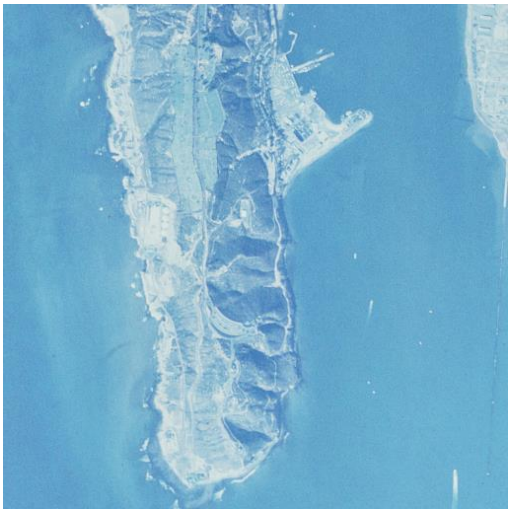

b

Fig. 2. Images Frisco (a) and Point Loma (b) used in experiments

$PSNR_{tc}$(UBMAD) starts from 28 dB which corresponds to PSNR of $\mathbf{I}^n$ with respect to $\mathbf{I}^t$. Then, if UBMAD increases, $PSNR_{tc}$ decreases but there are local maxima for UBMAD of about 280. $PSNR\text{-}HA_{tc}$(UBMAD) is characterized by steadily decreasing behavior without local maxima, i.e. visual quality of compressed images reduces if UBMAD decreases.

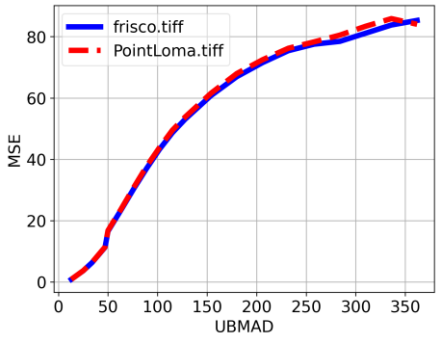

a

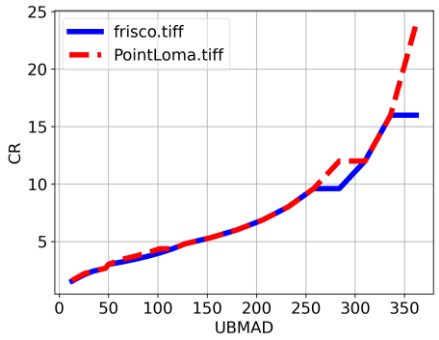

b

Fig. 3. Dependencies MSE_{nc}(UBMAD) (a) and CR(UBMAD) (b) for DAT-based compression applied to noisy images in Fig. 2 corrupted by AWGN with noise variance equal to 144

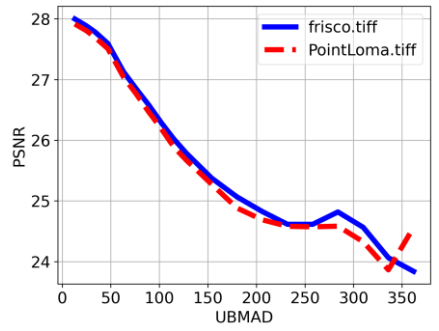

a

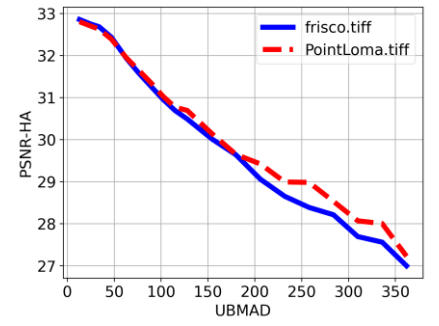

b

Fig. 4. Rate/distortion curves $PSNR_{tc}$(UBMAD) (a) and PSNR-HA_{tc}(UBMAD) (b) for the DAT-based compression applied to noisy images in Fig. 2 corrupted by AWGN with noise variance equal to 100

Since any visual quality metric is not perfect [27-29], it is worth using, in addition, to PSNR-HA, some other good visual quality metric. For this purpose, let us use MDPI [30, 31]. Note that MDSI varies in the limits from 0 for perfect quality to about 0.6 (very poor visual quality).

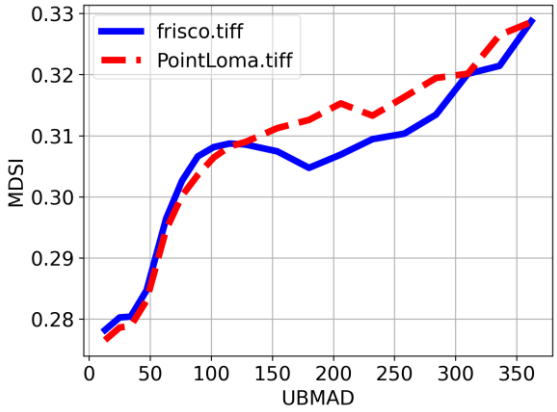

Fig. 5. Rate/distortion curves $MDSI_{tc}$(UBMAD) for the DAT-based compression applied to noisy images in Fig. 2 corrupted by AWGN with noise variance equal to 100

The plot analysis shows that although OOP is formally absent for the metric MDSI (Fig. 5). However, there is an interval of "flat" behavior or even local minimum neighborhood observed for UBMAD of about 200. Thus, if it is strongly desired to provide a rather high CR (for example, about 10, see Fig. 3,b), it can be recommended to set UBMAD≈200 (for a given $\sigma^2 = 100$).

Consider now the case of a slightly larger variance of AWGN ($\sigma^2 = 144$). Rate/distortion curves $PSNR_{tc}$(UBMAD) (a) and PSNR-HA_{tc}(UBMAD) are given in Fig. 6. The RDC $PSNR_{tc}$(UBMAD) (Fig. 6,a) starts from $PSNR_{tc}$≈26.5 dB and has local maxima or quasi-flat interval at UBMAD≈280. Meanwhile, formally OOP does not exist. Similarly to the plots in Fig. 4,b, the plots PSNR-HA_{tc}(UBMAD) (Fig. 6,b) have, in general, the decreasing, but "staircase-like" behavior.

Fig. 7 presents the rate/distortion curves $MDSI_{tc}$(UBMAD). Again, OOP is formally absent. However, there is a rather large interval of quasi-constant values with the "central" value of UBMAD≈250 that can be recommended for practical use if it is an ultimate goal to provide a large CR with a reasonably good quality of compressed images.

Finally, Fig. 8 shows the plots MAD_{tc}(UBMAD). As one can see, OOP formally exists and this happens for UBMAD of about 300 (although jumps of MAD are observed). We associate the OOP presence according to MAD since DAT-based compression has been designed to minimize and control MAD (in opposite to other compression techniques designed to minimize MSE).

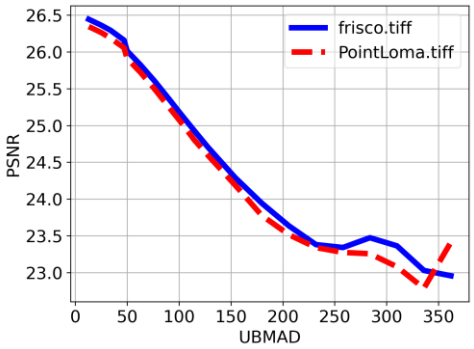

a

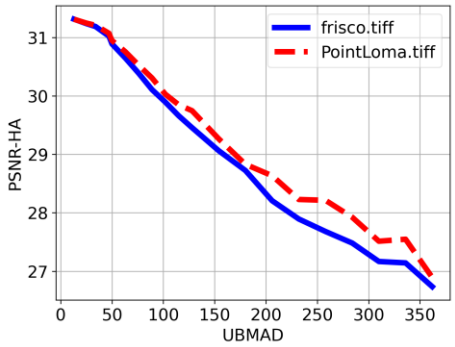

b

Fig. 6. Rate/distortion curves $PSNR_{tc}$(UBMAD) (a) and $PSNR\text{-}HA_{tc}$(UBMAD) (b) for the DAT-based compression applied to noisy images in Fig. 2 corrupted by AWGN with noise variance equal to 144

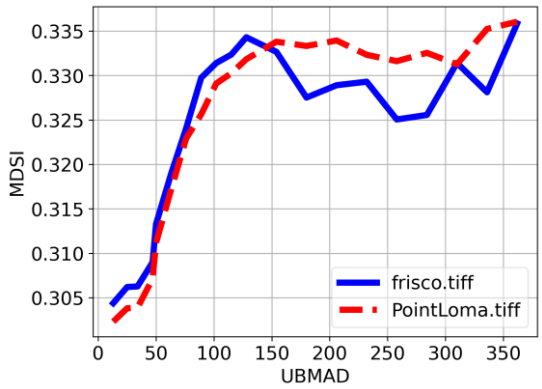

Fig. 7. Rate/distortion curves $MDSI_{tc}$(UBMAD) for the DAT-based compression applied to noisy images in Fig. 2 corrupted by AWGN with noise variance equal to 144

Fig. 9, a presents the noisy image and Fig. 9, b shows this image compressed with optimal UBMAD=206. As one can see, noise is clearly visible in Fig. 9,a, especially in homogeneous regions that correspond to water surface. It is sufficiently suppressed in the compressed image (Fig. 9,b) although some residual noise is visible. Fig. 10 gives another example. Noise intensity is larger here and noise is more annoying (Fig. 10,a). Compression with UBMAD=258 (Fig. 10,b) produces quite efficient noise suppression, although some smearing takes place too.

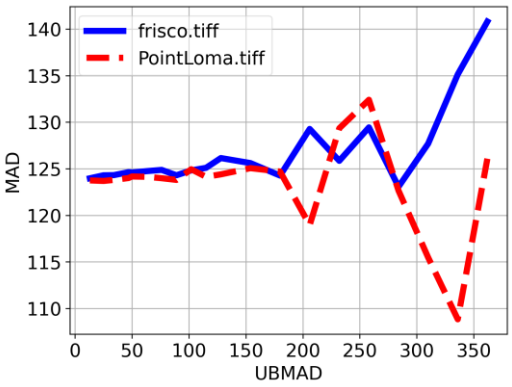

Fig. 8. Rate/distortion curves MAD_{tc}(UBMAD) for the DAT-based compression applied to noisy images in Fig. 2 corrupted by AWGN with noise variance equal to 144

a

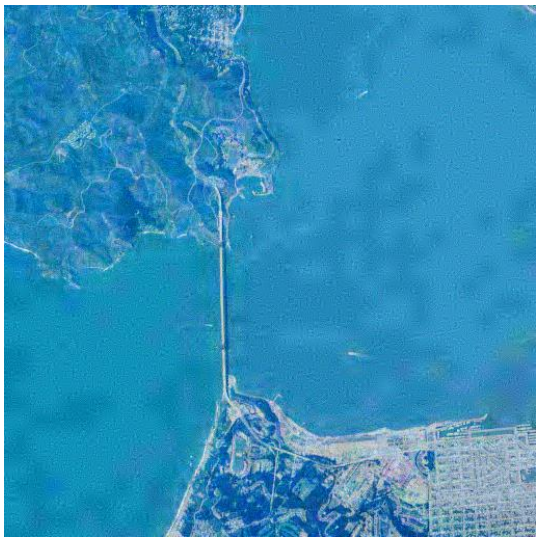

b

Fig. 9. Examples of noisy image Frisco, σ^2=100 (a) and compressed with optimal UBMAD=206 (b)

a

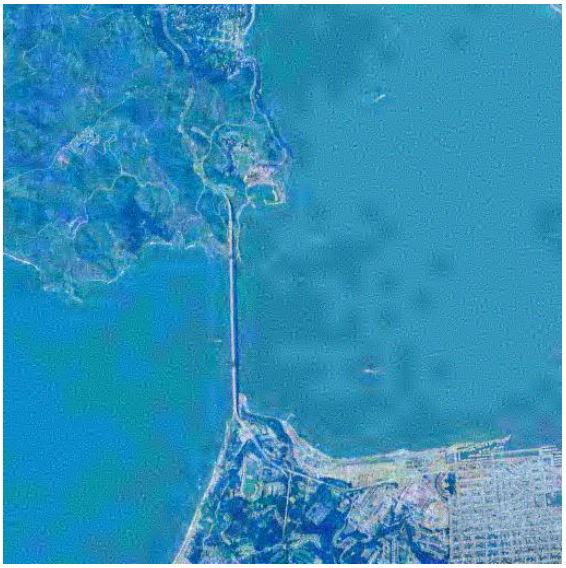

b

Fig. 10. Examples of noisy image Frisco, noise variance is equal to 144 (a) and compressed image, optimal UBMAD is equal to 258

Conclusions

The task of noisy image lossy compression using the DAT-based approach is considered. It is shown that the noise-filtering effect is observed if UBMAD is set properly. OOP has not been formally observed for PSNR and some considered visual quality metrics although local maxima or minima of rate/distortion curves have been found. Meanwhile, OOP is observed according to the MAD criterion (metric) that has not been earlier studied in the analysis of lossy compression applied to noisy images.

Contributions of authors: conceptualization – **Vladimir Lukin, Viktor Makarichev;** methodology – **Vladimir Lukin;** formulation of tasks – **Viktor Makarichev;** analysis – **Bogdan Kovalenko;** development of model – **Bogdan Kovalenko;** software – **Viktor Makarichev, Bogdan Kovalenko;** verification – **Bogdan Kovalenko, Vladimir Lukin;** analysis of results – **Viktor Makarichev, Bogdan Kovalenko;** visualization – **Bogdan Kovalenko;** writing – original draft preparation – **Bogdan Kovalenko;** writing – review and editing – **Vladimir Lukin.**

All the authors have read and agreed to the published version of the manuscript.

References

1. Kussul, N., Lavreniuk, M., Shelestov, A., Skakun, S. Crop inventory at regional scale in Ukraine: Developing in season and end of season crop maps with multi-temporal optical and SAR satellite imagery. *European Journal of Remote Sensing*, 2018, vol. 51, iss. 1, pp. 627-636. DOI: 10.1080/22797254.2018.1454265.

2. Mielke, C., Boshce, N. K., Rogass, C., Segl, K., Gauert, C., Kaufmann, H. Potential Applications of the Sentinel-2 Multispectral Sensor and the ENMAP hyperspectral Sensor in Mineral Exploration. *EARSeL eProceedings*, 2014, no. 13, iss. 2, pp. 93-10. DOI: 10.12760/01-2014-2-07.

3. Bioucas-Dias, J. M., Plaza, A., Camps-Valls, G., Scheunders, P., Nasrabadi, N., Chanussot, J. Hyperspectral Remote Sensing Data Analysis and Future Challenges. *IEEE Geoscience and Remote Sensing Magazine*, 2013, vol. 1, pp. 6-36. DOI: 10.1109/MGRS.2013.2244672.

4. Zhong, P., Wang, R. Multiple-Spectral-Band CRFs for Denoising Junk Bands of Hyperspectral Imagery. *IEEE Transactions on Geoscience and Remote Sensing*, 2013, no. 51, iss. 4, pp. 2269-2275. DOI: 10.1109/TGRS.2012.2209656.

5. Aiazzi, B., Alparone, L., Baronti, S. et al. Spectral distortion in lossy compression of hyperspectral data. *Journal of Electrical Computer Engineering*, 2012, vol. 2012. DOI: 10.1155/2012/850637.

6. Oh, H., Bilgin, A., Marcellin, M. Visually lossless JPEG 2000 for remote image browsing. *Information*, 2016, vol. 7, iss. 3, article no. 45. DOI: 10.3390/info7030045.

7. Zabala, A., Pons, X., Díaz-Delgado, R., Garcia, F., Auli-Llinas, F., Serra-Sagrista, J. Effects of JPEG and JPEG2000 lossy compression on remote sensing image classification for mapping crops and forest areas. *Proceedings of 2006 IEEE International Symposium on Geoscience and Remote Sensing*, 2006, pp. 790-793, DOI: 10.1109/IGARSS.2006.203.

8. Hussain, A. J., Al-Fayadh, A., Radi, N. Image compression techniques: A survey in lossless and lossy algorithms. *Neurocomputing*, 2018, vol. 300, pp. 44-69, DOI: 10.1016/j.neucom.2018.02.094.

9. Sayood, K. *Introduction to data compression*. San Francisco, Morgan Kaufmann Publ., 2017. 680 p.

10. Liu, H., Zhang, Y., Zhang, H., Fan, C., Kwong, S., Kuo, J., Fan, X. Deep learning-based picture-wise just noticeable distortion prediction model for image compression. *IEEE Transactions on Image Processing*, 2019, vol. 29, pp. 641-656. DOI: 10.1109/TIP. 2019.2933743.

11. Li, F., Krivenko, S., Lukin, V. Two-step providing of desired quality in lossy image compression by SPIHT. *Radioelectronic and computer systems*, 2020, no. 2, pp. 22-32. DOI: 10.32620/reks.2020.2.02.

12. Ozah, N., Kolokolova, A. Compression improves image classification accuracy. *Proceedings of Canadian Conference on Artificial Intelligence*, 2019, pp. 525-530. DOI: 10.1007/978-3-030-18305-9_55.

13. Said, A., Pearlman, W. A new fast and efficient image codec based on the partitioning in hierarchical trees. *IEEE Trans. on Circuits Syst. Video Technology*, 1996, vol. 6, pp. 243-250. DOI: 10.1109/76.499834.

14. Yee, D., Soltaninejad, S., Hazarika, D., Mbuyi, G., Barnwal, R., Basu, A. Medical image compression based on region of interest using better portable graphics (BPG). *Proceedings of 2017 IEEE International Conference on Systems, Man, and Cybernetics (SMC)*, 2017, pp. 216-221. DOI: 10.1109/SMC.2017.8122605.

15. Makarichev, V., Vasilyeva, I., Lukin, V., Vozel, B., Shelestov, A., Kussul, N. Discrete Atomic Transform-Based Lossy Compression of Three-Channel Remote Sensing Images with Quality Control. *Remote Sensing*, 2022, vol. 14, 125 p. DOI: 10.3390/rs14010125.

16. Siqueira, I., Correa, G., Grellert, M., Rate-Distortion and Complexity Comparison of HEVC and VVC Video Encoders. *Proceedings of the 2020 IEEE 11th Latin American Symposium on Circuits & Systems*, San Jose, Costa Rica, 2020, pp. 1-4. DOI: 10.1109/ LASCAS45839.2020.9069036.

17. Makarichev, V., Lukin, V., Illiashenko, O., Kharchenko, V. Digital Image Representation by Atomic Functions: The Compression and Protection of Data for Edge Computing in IoT Systems. *Sensors*, 2022, vol. 22, article id: 3751. DOI: 10.3390/s22103751.

18. Aiazzi, B., Alparone, L., Baronti, S., Lastri, C., Santurri, L., Selva, M. Tradeoff between radio-metric and spectral distortion in lossy compression of hyperspectral imagery. *Proc. SPIE 5208, Mathematics of Data/Image Coding, Compression, and Encryption VI, with Applications*, 2004, vol. 5208. DOI: 10.1117/12.508498.

19. Mullissa, A. G., Persello, C., Tolpekin, V. Fully Convolutional Networks for Multi-Temporal SAR Image Classification. *In Proceedings of the IGARSS 2018*, 2018, pp. 6635–6638. DOI: 10.1109/IGARSS.2018.8518780.

20. Wang, W., Zhong, X., Su, Z. On-Orbit Signal-to-Noise Ratio Test Method for Night-Light Camera in Luojia 1-01 Satellite Based on Time-Sequence Imagery. *Sensors*, 2019, no. 19, article id: 4077. DOI: 10.3390/s19194077.

21. Guo, Y., Bi, Q., Li, Y., Du, C., Huang, J., Chen, W., Shi, L., Ji, G. Sparse Representing Denoising of Hyperspectral Data for Water Color Remote Sensing. *Applied Sciences*, 2022, vol. 12, no. 15, article id: 7501. DOI: 10.3390/app12157501.

22. Al-Shaykh, O. K., Mersereau, R. M. Lossy Compression of Noisy Images. *IEEE Transactions on Image Processing*, 1998, vol. 7, no. 12, pp. 1641-1652. DOI: 10.1109/83.730376.

23. Chang, S. G., Yu, B., Vetterli, M. Adaptive wavelet thresholding for image denoising and compression. *IEEE Transactions on Signal Processing*, 2000, vol. 9, no. 9, pp. 1532-1546. DOI: 10.1109/83.862633.

24. Lukin, V., Zemliachenko, A., Abramov, S., Vozel, B., Chehdi, K. Automatic Lossy Compression of Noisy Images by Spiht or Jpeg2000 in Optimal Operation Point Neighborhood. *In Proceedings of the 2016 6th European Workshop on Visual Information Processing (EUVIP)*, Marseille, France, 2016, pp. 1–6. DOI: 10.1109/EUVIP.2016.7764581.

25. Zemliachenko, A. N., Abramov, S. K., Lukin, V. V., Vozel, B., Chehdi, K. Lossy Compression of Noisy Remote Sensing Images with Prediction of Optimal Operation Point Existence and Parameters. *Journal of Applied Remote Sensing*, 2015, vol. 9, iss. 1, article id: 095066. DOI: 10.1117/1.JRS.9.095066.

26. Ponomarenko, N., Ieremeiev, O., Lukin, V., Egiazarian, K., Carli, M. Modified Image Visual Quality Metrics for Contrast Change and Mean Shift Accounting. *Proceedings of CADSM*, 2011, pp. 305 - 311.

27. Rajkumar, S., Malathi, G. A Comparative Analysis on Image Quality Assessment for Real Time Satellite Images. *Indian Journal of Science and Technology*, 2016, vol. 9, iss. 34, pp. 1-11. DOI: 10.17485/ijst/2016/v9i34/96766.

28. Zhao, Y., Zhang, Y., Han, J., Wang, Y. Analysis of Image Quality Assessment Methods for Aerial Images. *The 10th International Conference on Computer Engineering and Networks*, 2020, vol. 1274, pp. 168-175. DOI: 10.1007/978-981-15-8462-6_19.

29. Zheng, R., Jiang, X., Ma, Y., Wang, L. A Comparison of Quality Assessment Metrics on Image Resolution Enhancement Artifacts. *2022 International Conference on Culture-Oriented Science and Technology*, 2022, pp. 200-204. DOI: 10.1109/CoST57098.2022.00049.

30. Nafchi, H. Z., Shahkolaei, A., Hedjam, R., Cheriet, M. Mean Deviation Similarity Index: Efficient and Reliable Full-Reference Image Quality Evaluator.

IEEE Access, 2016, vol. 4, pp. 5579–5590. DOI: 0.1109/ACCESS.2016.2604042.

31. Zhong, M., Chen, J., Niu, Y. Weighted Mean Deviation Similarity Index for Objective Omnidirectional Video Quality Assessment. *Parallel Architectures, Algorithms and Programming*, 2019, vol. 1163, pp. 109-117. DOI: 10.1007/978-981-15-2767-8_10.

Надійшла до редакції 05.01.2023, розглянута на редколегії 17.04.2023

ПОПЕРЕДНІЙ АНАЛІЗ СТИСНЕННЯ З ВТРАТАМИ ЗОБРАЖЕНЬ З ШУМОМ КОДЕРОМ НА ОСНОВІ ДИСКРЕТНОГО АТОМАРНОГО ПЕРЕТВОРЕННЯ

В. О. Макарічев, Б. В. Коваленко, В. В. Лукін

Дистанційне зондування надає дані (зображення), важливі для багатьох сучасних додатків. Кількість зображень і їх середній розмір мають тенденцію до зростання. Це ускладнює їх передачу по лініях зв'язку, зберігання та розповсюдження. Таким чином, бажано застосовувати стиснення, причому переважно використовується стиснення з втратами. Більшість методів стиснення з втратами базуються на припущенні, що зображення не містять шуму. Тим часом, зображення часто мають шум, і це слід враховувати при розробці та аналізі ефективності методів стиснення зображень. Стиснення з втратами вже вивчалося для кількох кодерів. Однак не було досліджено нещодавно запропоновані методи на основі атомарного перетворення, які мають низку переваг, зокрема, здатність забезпечувати конфіденційність стиснутих даних. Основною темою цієї статті є особливості стиснення зашумленого зображення з втратами за допомогою кодера на основі атомарного перетворення. Наша мета – проаналізувати, чи забезпечує розглянутий метод стиснення ефект фільтрації шумів і так звану оптимальну робочу точку. Завдання полягає в тому, щоб отримати криві рівня спотворень від параметрів стиснення для кодера на основі атомарного перетворення, який застосовано до зашумлених зображень, і проаналізувати їх поведінку для кількох характеристик ефективності, таких як показники якості та ступінь стиснення. У першу чергу нас цікавить монотонність основних залежностей. Основні результати наступні. По-перше, показано, що залежності мають немонотонний характер і можлива поява аналогів оптимальної робочої точки принаймні для такої метрики як максимальна абсолютна похибка. По-друге, існує певна поведінка залежності ступеня стиснення від параметра UBMAD, який контролює стиснення. Були проведені експерименти для кількох тестових зашумлених зображень різної складності та шумів різної інтенсивності. В якості висновків показано, що розглянутий кодер може мати оптимальні робочі точки для зображень, які мають досить просту структуру. Однак на даний момент важко передбачити їх існування та відповідні параметри кодера.

Ключові слова: стиснення з втратами; атомарні перетворення; крива спотворення-швидкість; оптимальна робоча точка.

Макарічев Віктор Олександрович – канд. фіз.-мат. наук, докторант каф. комп'ютерних систем, мереж і кібербезпеки, Національний аерокосмічний університет ім. М. Є. Жуковського «Харківський авіаційний інститут», Харків, Україна.

Коваленко Богдан Віталійович – асп. каф. інформаційно-комунікаційних технологій ім. О. О. Зеленського, Національний аерокосмічний університет ім. М. Є. Жуковського «Харківський авіаційний інститут», Харків, Україна.

Лукін Володимир Васильович – д-р техн. наук, проф., зав. каф. інформаційно-комунікаційних технологій ім. О. О. Зеленського, Національний аерокосмічний університет ім. М. Є. Жуковського «Харківський авіаційний інститут», Харків, Україна.

Viktor Makarichev – Candidate of Physico-Mathematic Science, Doctoral Student of the Department of Computer Systems, Networks, and Cyber Security, National Aerospace University “Kharkiv Aviation Institute”, Kharkiv, Ukraine,
e-mail: v.makarichev@khai.edu, ORCID: 0000-0003-1481-9132.

Bogdan Kovalenko – Ph.D. student of the Department of Information-communication Technologies named after O. O. Zelensky, National Aerospace University “Kharkiv Aviation Institute”, Kharkiv, Ukraine,
e-mail: b.kovalenko@khai.edu, ORCID: 0000-0002-9360-0691.

Vladimir Lukin – Doctor of Technical Science, Professor, Head of the Department of Information-communication technologies named after O. O. Zelensky, National Aerospace University “Kharkiv Aviation Institute”, Kharkiv, Ukraine,
e-mail: v.lukin@khai.edu, ORCID: 0000-0002-1443-9685.